17th World Conference on Earthquake Engineering, 17WCEE
Sendai, Japan - September 13th to 18th 2020

SUBASSEMBLAGE TEST OF NATRUALLY BUCKLING BRACES UNDER FAR-FIELD AND NEAR-FAULT CYCLIC LOADINGS

P.C. Hsiao[(1)], Y.T. Cheng[(2)]

[(1)] *Assistant Professor, National Taiwan University of Science and Technology, Taiwan, pchsiao@mail.ntust.edu.tw*
[(2)] *Graduate Student, National Chung Hsing University, Taiwan*

Abstract

Naturally buckling braces (NBBs) has been previously developed through tying two channel segments using different steel grades and a design of intended eccentricity along the brace length. The developed NBBs forming a novel mechanism were experimentally verified to provide a stable and ductile hysteretic behavior with the features of early yielding, large post-yield stiffness in tension and well-postponed local buckling in compression compared to conventional buckling braces. In the study, a number of chevron NBB specimens have been tested to investigate the effects of brace angles, member and local slenderness ratios and steel grades of the low-yield segment. Two types of cyclic loading protocols, including far-field and near-fault cyclic loadings, were applied, and the results were investigated and compared to clarify the seismic performance of NBBs with various brace member slenderness under near-fault earthquakes. The test results verified that the chevron NBBs provided a comparable and ductile hysteretic behavior in tension and compression under both far-field and near-fault cyclic loading protocols. An approach to simplified the measured strength backbone curves to bi-linear strength curves was proposed to define the yield strength of the chevron NBB specimens. A formula was then developed to accurately estimate the level of the strength degradation of the chevron NBBs according to the member and local slenderness ratios of the braces. With small width-to-thickness ratio of low-yield segment and sufficient rigidity of the end plate, the chevron NBB specimens presented a good fatigue life with a CPD value greater than 450.

Keywords: steel braces, slenderness, cyclic loading protocol, near-fault earthquakes

1. Introduction

Naturally buckling braces (NBB) have been developed upon two design ideas of composite member using two channel segments of different steel grades and an intended eccentricity [1]. The NBBs provide an alternative of steel braces in the special concentrically braced frames (SCBF). The mechanism of NBBs has been experimental verified to form a more ductile and stable hysteretic behavior compared to the conventional buckling braces [1, 2]. The previous experiments have shown that the hysteretic behavior of a single NBB had large tensile strengths with large post-yield stiffness while the compressive strengths were relatively small due to member buckling of the brace. The difference mechanism in tension and compression forms an incomparable hysteretic behavior in tension and compression, including strength and stiffness. However, it is still unknown that if various loading history would affect or change the seismic performance of NBBs due to the incomparable behavior in the tension and compression. No previous research has tested the NBBs in V-shape or chevron bracing configuration, where one brace is subjected to the loading beginning with tension while the other is subjected to the loading beginning with compression. The seismic performance of a pair of NBBs needs to be experimentally verified. Moreover, the seismic performance of NBBs under near-fault loading protocol is still unknown and needs to be clarified.

The study tested a series of half-scaled chevron NBB specimens to examine the seismic performance of NBBs in chevron configuration and compare that under far-field and near-fault cyclic loadings. Among the specimens, various brace angles, slenderness ratios, width-to-thickness ratios and steel grades of the low-yield segment have been covered and compared. In this paper, the measured results are evaluated in following several aspects, including strength backbone curves, strength degradation, and fatigue life. The effect of strength degradation of NBBs is related to the member and local slenderness ratios of specimens in the study, and a formula was established to estimate the levels of the strength degradation according to the member and local slenderness ratios.

2. Test Program and Design of Specimens

Six half-scaled chevron NBB specimens, including a total of twelve braces, have been designed and tested. Each pair of NBBs were tested using the test setup as shown in Fig. 1. The horizontal cyclic loading was applied by a 2000 kN actuator to the inclined braces through a loading column having a pinned end at the column base as shown in the figure. The height of the working point of the braces was 1799 mm, and the lateral load was applied at a height of 2120 mm from the floor beam. A lateral support frame system was arranged at top of the loading column to prevent out of plane displacement of the column. Among specimens as listed in Table 1, chevron braces with brace angles of 45 and 30 degrees, i.e. A45S15 and A30S15, were designed to provide the same level of lateral load capacities, about 900 kN. It led to different lengths and cross sections, which therefore resulted in different member and local slenderness ratios as shown in Table 1 and Fig. 2. All dimensional variables are illustrated in Fig. 1, when b is calculated by B-2tLY and r_{com} is the radius of gyration of the overall cross section as shown in Fig. 1. The steel grades of SS400 and SM570C was adopted for the low-yield and high-strength channel segments. Two types of cyclic loading protocols, far-field and near-fault types as shown in Fig. 3, were applied for specimens. A45S15 and A30S15 are denoted as the tests subjected to far-field loading protocol, while A45S15-N and A30S15-N are denoted as that subjected to near-fault loading protocol. Specimen A45S08 has identical dimensions with A45S15 but reducing the thickness of low-yield segment from 15 mm to 8 mm to examine the influence of the width-to-thickness ratios. Specimen A45L08 has identical dimensions with A45S08 but adopting LYS100 steel for the low-yield segment to evaluate the effect of the yield strength of the low-yield segment. The loading sequence for beam-to-column moment connections in special moment resisting frames [3, 4] with additional four cycles of 0.125% story drift was adopted as the far-field cyclic loading in the study, while SAC Near-fault loading protocol for special moment resisting frames [3] was used as the near-fault cyclic loading.

Table 1 – Chemical composition of cement samples

Specimen	Brace angle (degree)	$B \times D$ (mm)	L (mm)	L_{diss} (mm)	t_{LY} (mm)	t_{HS} (mm)	Applied Loading	b/t_{LY}	KL/r_{com}
A45S15	45	120×120	1924	1624	15	15	Far-field	6	40.3
A45S15-N	45	120×120	1924	1624	15	15	Near-fault	6	40.3
A30S15	30	150×150	1342	1042	15	15	Far-field	8	22.0
A30S15-N	30	150×150	1342	1042	15	15	Near-fault	8	22.0
A45S08	45	120×120	1924	1624	8	15	Far-field	13	40.7
A45L08	45	120×120	1924	1624	8	15	Far-field	13	40.7

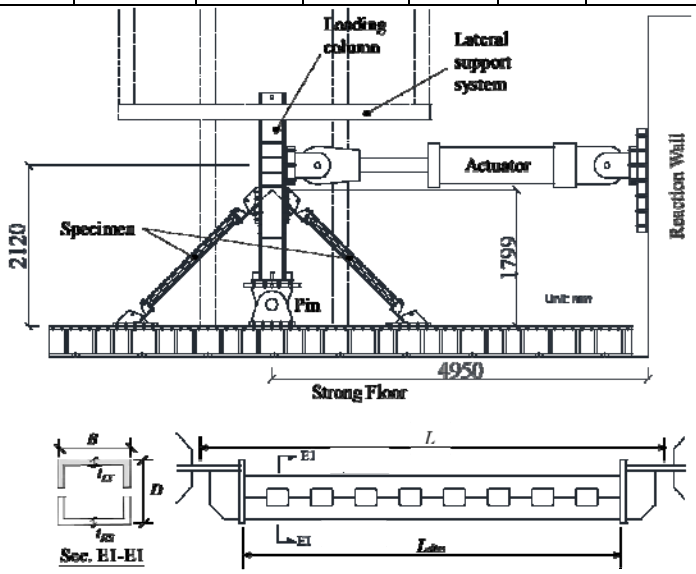

Fig. 1 – Illustration of test setup and NBB specimens

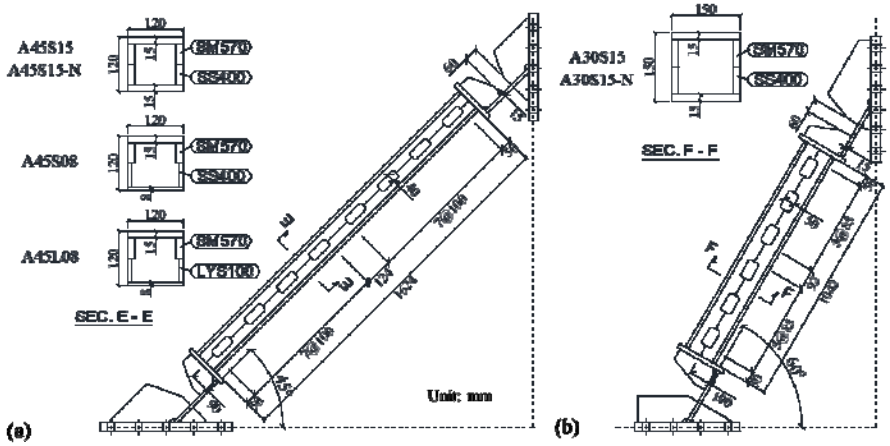

Fig. 2 – Detailed dimensions of the specimens with brace angles of (a) 45 and (b) 60 degree.

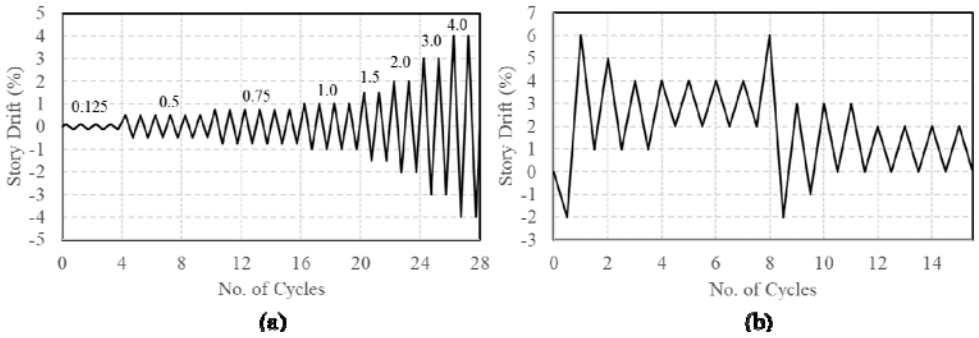

Fig. 3 – Adopted cyclic loading protocols: (a) Far-field and (b) Near-fault.

3. Test Results and Observations

The measured hysteretic results are shown in Figs. 4 to 6. The overall lateral displacements of the chevron NBB specimens shown in the figures were measured at the working point of braces in the tests through wire-type displacement transducers. The measured load of the actuator was transferred to the corresponding lateral load at the height of working point level by the principle of leverage of the loading column for the shown hysteretic responses. It is shown that the local buckling was successfully postponed until at least 3% story drift in the specimens subjected to far-field cyclic loading, and no strength degradation was shown prior to the occurrence of the local buckling. With relatively small width-to-thickness ratio, the strength degradation of A45S15 beyond the occurrence of local buckling was not significant (Fig. 4a), when significant strength degradation was shown in A45S15-N under near-fault loading protocol (Fig. 4b) even before the occurrence of the local buckling. No local buckling and strength degradation was observed in A30S15 having brace angle of 30 degrees, while yielding of the end plates between the knife plate connection and brace member was observed beyond the cycles of 3% story drift (Fig. 4c). Similarly, negligible strength degradation was shown in A30S15-N under near-fault loading protocol (Fig. 4d). Since no fracture or severe loss of the strength occurred at the end of the cyclic loading protocols, fatigue cycles at 3% story drift level were continuously conducted until meeting apparent fracture to examine the fatigue life of the specimens. Since no apparent failure was shown in the two specimens subjected to near-fault cyclic loading, it is verified that the chevron NBBs enabled to provide sufficient ductility for facing near-fault seismic loads.

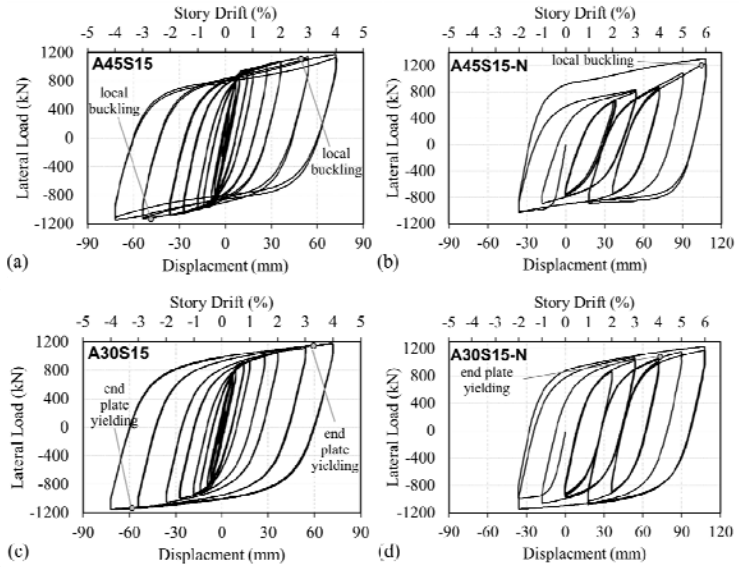

Fig. 4 – Measured hysteretic responses of (a)A45S15, (b)A45S15-N, (c)A30S15, and (d)A30S15-N

Similar with A45S15, A45S08 which had smaller thickness of the low-yield segment met local buckling during the cycles at 3% story drift level as shown in Fig. 5a. Since A45S08 had greater width-to-thickness ratio of the low-yield segment, however, deformation concentration rapidly turned severe beyond the onset of local buckling which led to significant strength degradation. The test was terminated due to the occurrence of weld fracture. A45L08 showed very similar seismic performance with A45S08 but earlier yielding, greater strain hardening and smaller overall strengths due to the use of LYS100 steel

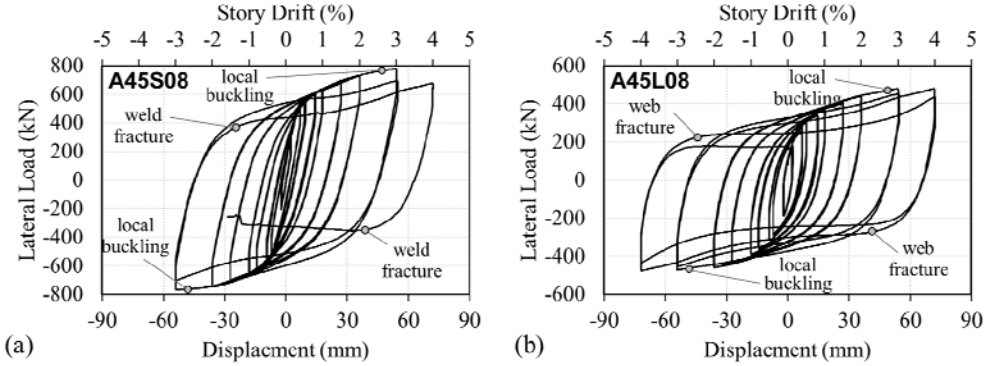

Fig. 5 – Measured hysteretic responses of (a)A45S08, and (b)A45L08

4. Effect of Strength Degradation

Various levels of the strength degradation were observed in the measured responses among specimens as mentioned above. Among four specimens subjected to far-field cyclic loading in the study, the degradation of hysteretic loops in the cycles of 3% story drift, where local buckling usually occurred as mentioned earlier, was found representative to show the level of the strength degradation for each specimen. Fig. 6a shows the measured hysteretic loops of two cycles of 3% story drift of A45S08 as an example. The strength in the second cycle was degraded and thereby caused reduced energy dissipation. The levels of the strength degradation were therefore defined as the ratio of dissipated energy in the first 3%-story-drift cycle ($E_{3\%\_1st}$) to that in the second 3%-story-drift cycle ($E_{3\%\_2nd}$) for each specimen. The resulting energy ratios of $E_{3\%\_2nd}$ /$E_{3\%\_1st}$ were shown plotted with the local slenderness ratios (b/t_{LY}) and member slenderness ratios (KL/r_{com}) among specimens as shown in Figs. 6b and 6c, respectively. It shows that the increase of the local and member slenderness ratios would lead to reduction on the energy ratios of $E_{3\%\_2nd}$ /$E_{3\%\_1st}$. It is considered that the strength degradation of specimens was caused by following two reasons. First, the residual deformations/deflections along the brace length after the formation of plastic hinges caused the reduction of the axial strength of NBBs in both tension and compression. Figure 7 shows the residual deformations/deflections of A45S15 and A30S15 at zero story drift after the completion of the first 4% story drift cycle. It is apparent that the NBBs with larger member slenderness ratios (KL/r_{com}) presented greater residual deformations/deflections. Second, the occurrence of local buckling results in severe strain concentration at mid-span of the brace and thereby caused the reduction of the axial strength of NBBs in both tension and compression. The strength degradation would be mitigated by the use of smaller local slenderness ratios (b/t_{LY}) upon the test observation. A regression equation was therefore developed to estimate the energy ratios of $E_{3\%\_2nd}$ /$E_{3\%\_1st}$. by the local and member slenderness ratios, as shown in Eq. 1 upon the test results above.

$$\frac{E_{3\%\_1st}}{E_{3\%\_2nd}} = 171\% \cdot \left(\frac{b}{t_{LY}}\right)^{-0.08} \left(\frac{KL}{r_{com}}\right)^{-0.12} \quad (1)$$

Figure 8 shows the accuracy of Eq. 1 to estimate the energy ratios of $E_{3\%\_2nd}$ /$E_{3\%\_1st}$ compared to the measured responses. It should be noted that a value of $E_{3\%\_2nd}$ /$E_{3\%\_1st}$ close to 100% is suggested to prevent apparent strength degradation under near-fault loading protocol based on the results in the study. It should be considered in the design of the chevron NBBs.

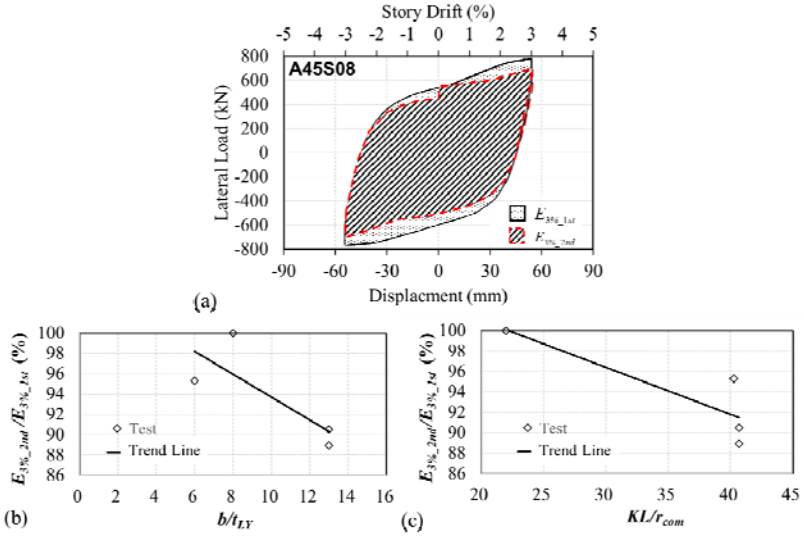

Fig. 6 – (a) Hysteretic loops of A45S08 in the two cycles of 3% story drift; Energy ratios of $E_{3\%\_2nd}/E_{3\%\_1st}$ with various (b) b/t_{LY} and (c) KL/r_{com} ratios

Fig. 7 – Residual deformations/deflections of (a) A45S15 and (b) A30S15 at zero story drift after the first cycle of 4% story drift

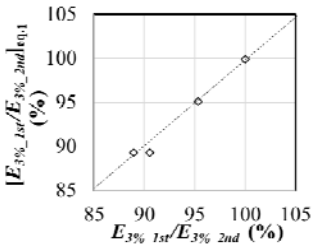

Fig. 8 – Accuracy of the Eq. 1

5. Fatigue Life

Fatigue life of the chevron NBB specimens had been evaluated through cumulative plastic deformation (CPD) and the total energy dissipation, En, before fracture failure of the specimens. Figures 9a and 9b show the resulting values of CPD and En of six specimens in the study, respectively. The results showed that A45S15 had CPD over 450, when the A45S15-N had CPD greater than 500. It implies that the loading history didn't have a significant impact on the values of CPD. A30S15 and A30S15-N showed relative small CPD values by 300 in average. It is considered due to the undesired yielding and fracture of the end-plate as mentioned earlier. The end plates were suggested to be strengthened by adding stiffeners to develop full ductility and CPD of the specimen. A45S08 and A45L08 had much smaller values of CPD resulted from the

occurrence of fracture at mid-span of braces by the end of the far-field loading protocol. It was regarded as a premature failure mode due to large local slenderness ratio of the specimens. Total energy dissipation of six specimens in the study shows a similar trend with resulting CPDs. It should be stated that more experimental investigation is still needed to verify the findings in the study.

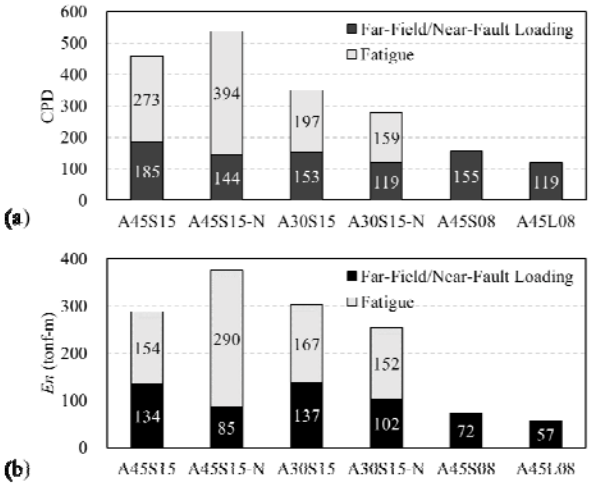

Fig. 9 – Fatigue life of specimens: (a) CPD, and (b) Total energy dissipation

6. Conclusions

A series of chevron NBB specimens have been experimentally investigated to clarify seismic performance under far-field and near-fault cyclic loadings. The test results verified that the chevron NBBs provided a comparable and ductile hysteretic behavior in tension and compression under both far-field and near-fault cyclic loading protocols. Local buckling was successfully postponed until at least story drift of 3% radians, while the main failure mode was the fracture at mid-span of the brace caused by severe local buckling. The measured results have been evaluated regarding several aspects, including strength backbone curve, strength degradation, and fatigue life. An approach to simplified the measured strength backbone curves to bi-linear strength curves was proposed to define the yield strength of the chevron NBB specimens. The strength degradation of NBBs was related to the member and local slenderness ratios of the specimens, and a formula was then developed to accurately estimate the level of the strength degradation according to the member and local slenderness ratios of the braces. It was also shown that with small width-to-thickness ratio of low-yield segment and sufficient rigidity of the end plate, the chevron NBB specimens presented a good fatigue life with a CPD value greater than 450.

7. References

[1] Hsiao PC, Hayashi K, Inamasu H, Luo YB, Nakashima M (2015): Development and Testing of Naturally Buckling Steel Braces. *J. of Structural Engineering*, ASCE, **142**(1).

[2] Inamasu H, Skalomenos KA, Hsiao PC, Hayashi K, Kurata M, Nakashima M (2017): Gusset Plate Connections for Naturally Buckling Braces. *J. of Structural Engineering*, ASCE, **143**(8).

[3] Krawinkler H, Gupta A, Medina R, Luco N (2000): Development of Loading Histories for Testing of Steel Beam-to-Column Assemblies. *SAC Background Report SAC/BD-00/10*.

[4] ANSI/AISC 341-16 (2016): Seismic Provisions for Structural Steel Buildings. *American Institute of Steel Construction*, Chicago (IL).

